

3.5 BROADENING OF CONVECTIVE CELLS DURING COLD AIR OUTBREAKS: A HIGH RESOLUTION STUDY USING A PARALLELIZED LES MODEL

Michael Schröter* and Siegfried Raasch

Institute of Meteorology und Climatology, University of Hannover, Germany

1 INTRODUCTION

Large-eddy simulation (LES) is used to study the broadening of mesoscale convective cells (MCC) during cold-air outbreak (CAOB) situations. Until today, there are still some open questions concerning basic features of organized convection during CAOBs. Whereas in classical laboratory experiments of Rayleigh-Bénard convection the aspect ratio of hexagonal cells (the ratio of the cell diameter to its height) is about 3, values between 10 and 30 are typically observed for MCC during CAOB-situations. For a comprehensive review about the phenomenon of MCC see Atkinson and Zhang (1996). In earlier numerical studies of CAOBs it was found that diabatic processes (latent heat release due to condensation, and especially radiative cooling) are an essential prerequisite for cell broadening and are thus responsible for these large aspect ratios (e.g. Müller and Chlond, 1996; Dörnbrack, 1997). Jonker et al. (1999a) turned out that only inert tracers appear to undergo cell broadening, whereas at the same time the dynamics including the buoyancy field do not broaden. They found that fluctuations grew most rapidly at a ratio of 1 between the entrainment flux and the surface flux of a tracer, in accordance with the findings of Dörnbrack (1997). Jonker et al. (1999b) showed using LES that in a cumulus topped boundary layer the moisture field in the sub-cloud layer tends to acquire dominating mesoscale fluctuations due to the positive flux ratio of moisture. These fluctuations have an impact on the overlaying cloud layer, in particular on the typical cloud size.

Nevertheless, some shortcomings remain from these studies due to the insufficient computer resources available at that time. An LES of MCC during a CAOB will need a computational domain of about 100 km^2 in order to allow for the development of the large cells. Simultaneously a grid resolution of about 50 to 100 m is necessary to resolve also the smaller energy containing eddies

of the CBL which might interact with the larger cells. Under these circumstances, the numerical grid requires about 10^8 grid points per each variable. Dörnbrack (1997) simulated the cell growth for a dry CBL between two plates, but the horizontal extent of his model domain was too small to follow the subsequent evolution of the cell broadening towards a stationary state. At the end of his LES, one convection cell filled out about one half of the box side and thus the domain size became too small to allow for a further growth of the cells. The same restrictions hold for Jonker et al. (1999b), where the simulated domain was only 6.4 km^2 in the horizontal. Müller and Chlond (1996) simulated a CAOB using LES in combination with a method for dynamically adapting domain size and resolution to the evolving structures. In order to bypass the computer memory problem, the horizontal size of their model domain and the horizontal resolution of the computational grid have been adjusted to the scale of the dominant convective structures. At the end of their runs, the horizontal domain extended over about $100 \times 100 \text{ km}^2$ but with a horizontal grid spacing of 1.6 km. Therefore, these simulations were unable to resolve the ordinary small scale convection and to consider possible interactions between the large scale structures and the small scale convective elements. Additionally, they had to use non-isotropic eddy diffusivity coefficients in order to account for the increasing anisotropy of the model grid. However, it is unclear if these non-isotropic diffusivities may itself affect the aspect ratio of the cells.

Today, for the first time, massively parallel computers allow the LES of a very large horizontal domain with fine grid spacing at one and the same time. We took this opportunity using the parallelized LES model PALM (Raasch and Schröter, 2001) to repeat the earlier studies mentioned above but avoiding their shortcomings. The model contains a water cycle with cloud formation and precipitation processes and it takes into account infrared radiative cooling in cloudy conditions. For a detailed description, particularly of the parallelization method, the reader is referred to Raasch and Schröter (2001) and to the

*Corresponding author address: Michael Schröter, Institut für Meteorologie und Klimatologie, Universität Hannover, Herrenhäuser Str. 2, 30419 Hannover, Germany; schroeter@muk.uni-hannover.de

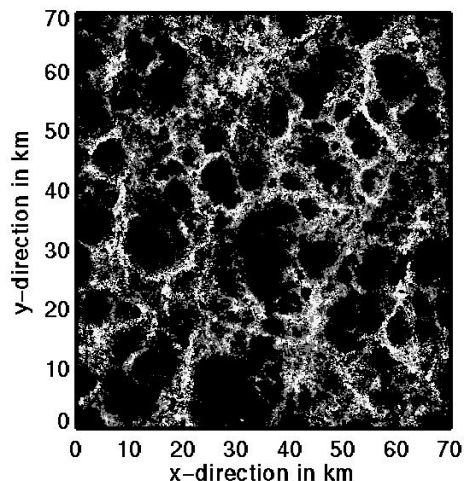
paper P3.13 in this preprint volume.

2 MODEL SETUP

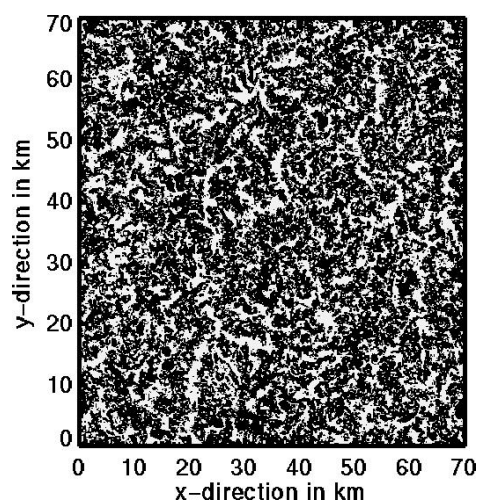
To study broadening of mesoscale convective cells we refer to a CAOB situation observed during ARKTIS 1991 experiment which has been already used as reference state by Müller and Chlond (1996), where further details of the experiment are described. We used the initialization according to this observed situation for two principal runs. For both runs the model domain covered an area of $70.4 \text{ km} \times 70.4 \text{ km}$ in the horizontal and approximately 5.5 km in the vertical direction. Using a grid spacing of 100 m in the horizontal and 50 m in the vertical direction (for $z > 3300 \text{ m}$ the vertical grid spacing was smoothly stretched) resulted in $704 \times 704 \times 80$ grid points. The demand on main memory was about 30 GBytes . Both runs covered a period of 12.5 h , which is more than 50 convective timescales. During the simulations, the ratio between the horizontal domain extension and the boundary layer height z_i decreased from 500 at the beginning to about 23 at the end of the runs (compared with 16 in the dry convection study of Dörnbrack, 1997). The first run (hereafter RUN1) includes the whole water cycle, whereas the second run (RUN2) takes the same initial parameters but the water cycle was switched off in order to examine the role of adiabatic heat sources in the cell broadening process. The simulations were performed on 256 PEs on a Cray-T3E LC 384. For RUN1 each PE required 115 CPU-hours (4.8 days) in total.

3 SIMULATION RESULTS

During RUN1 large scale convective cells develop. The signals of these cells can be very clearly identified by visual analysis. In Figure 1 cross sections in the x - y -plane through the field of liquid water q_l (1a) and the vertical velocity field w (1b) are shown for the middle of the cloud layer at the end of RUN1 ($t = 12.5 \text{ h}$). A striking signal of the MCC comes from the q_l -field (1a), which clearly resemble satellite pictures of MCC. The centers of the cells are represented by a homogeneous distribution of relatively large values of q_l . These centers are enclosed by narrow rings where small values of q_l are found. This kind of cellular pattern is typical for closed convective cells. The predominant diameters of the cells are about $20\text{-}30 \text{ km}$, which is in good agreement with the observations during ARKTIS 1991. Seemingly in accordance with the results of Dörnbrack (1997), the w -field



(a) q_l -field, $t = 12.5 \text{ h}$, $z = 3100 \text{ m}$



(b) w -field, $t = 12.5 \text{ h}$, $z = 2150 \text{ m}$

Figure 1: Contour plots of horizontal cross sections in the middle of the cloud layer of the liquid water content (a) and of the vertical velocity (b) for RUN1 at $t = 12.5 \text{ h}$. (a): white areas $q_l < 0.375 \text{ k kg}^{-1}$, dark areas $q_l > 0.425 \text{ k kg}^{-1}$; (b): white areas $w < 0.0$, dark areas $w > 0.0$.

in 1b does not show any organized pattern. On the first view, only spatially randomly-distributed updrafts (dark areas) and downdrafts (light areas) can be detected. However, on closer inspection cellular patterns can also be identified in the w -field, due to positive correlations with the field of liquid water. In areas of small liquid water content downdrafts predominantly occur, whereas in the

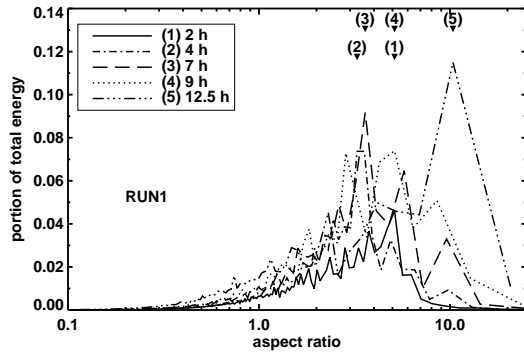


Figure 2: Vertical velocity power spectra for RUN1 resulting from two-dimensional Fourier analysis of x-y cross sections located in the middle of the developing cloud layer. An averaging of Fourier coefficients is performed in order to generate a one-dimensional presentation. Shown is the percentage of total energy as a function of the aspect ratio at different times. Aspect ratios of the corresponding dominating scales are marked by numbers and triangles.

center of the cells updrafts are more frequent than downdrafts. Hence, each mesoscale convection cell appears as an organized conglomeration of many randomly distributed up- and downdrafts. In contrast with this, the earlier study of Müller and Chlond showed a clearly cellular pattern in w , obviously caused by the much coarser grid resolution they used, whereas in Dörnbrack's study the detection of the mesoscale structure was prevented by the limited domain size.

The fact that in our simulation mesoscale structures not only occur in the scalar fields but also in the dynamic variables becomes evident from the power spectra of the vertical velocity as well. Figures 2 and 3 presents the power spectra of w at $0.5 z_i$ for different times as a function of the aspect ratio, which is defined here as the ratio between spectral wavelength and z_i . The broadening of the dominating scales is clearly visible by the temporal increase of the dominating aspect ratio. Until the end of the simulation the dominating aspect ratio increases from approximately 3.5 at 4 h and 7 h respectively to more than 10 at 12.5 h. These results are in agreement with the earlier findings of (Müller and Chlond, 1996), but our runs show much larger energy on the shorter wavelengths. However, they are in contrast with the results of Jonker et al. (1999b), who did not find a scale increase in the dynamic variables in their runs with limited domain size. This scale increase obviously takes place, if the domain size is large enough.

During RUN2, which was performed with con-

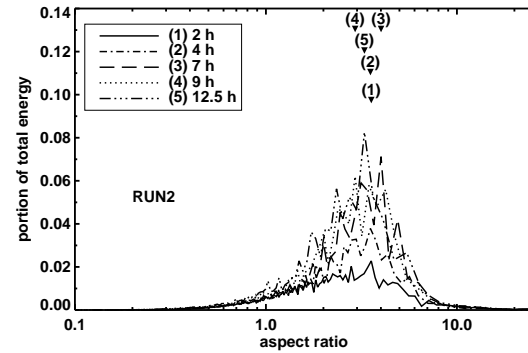


Figure 3: As Fig. 2 for RUN2.

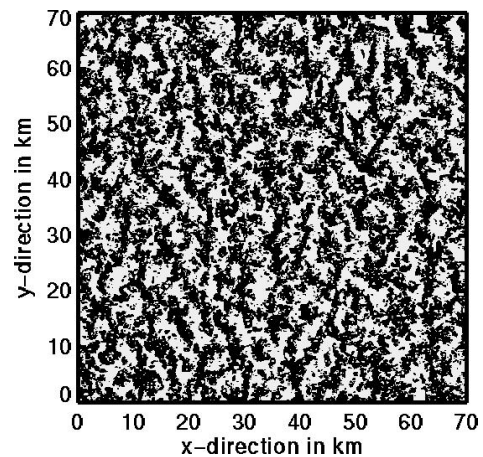


Figure 4: Contour plots of the vertical velocity in horizontal x-y-cross-sections for RUN2 at $t = 12.5$ h and $z = 1000$ m. White areas $w < 0.0$, dark areas $w > 0.0$.

densation and longwave radiation processes switched off, a formation of MCC does not take place. Figure 4 shows a cross-section through the w -field at $t = 12.5$ h. It is taken in the level, where the resolved variance of the vertical velocity reached its maximum. The distribution of up- and downdrafts and the aspect ratios observed during RUN2 agree with the ones detected in cloudless convective boundary layers. The power spectra of RUN2 (Figure 3) definitely elucidate that MCC does not occur. They do not show any growth of the dominating aspect ratio. Within the whole period of the simulation it remains between 3 and 3.5. Since the formation of mesoscale convective cells fails to appear in RUN2, our results support the earlier findings of Müller and Chlond (1996) that diabatic heat sources are responsible for existence and broadening of the cells. Nevertheless, thanks to the power of today's supercomputers, some of the uncertainties of these earlier investigations were re-

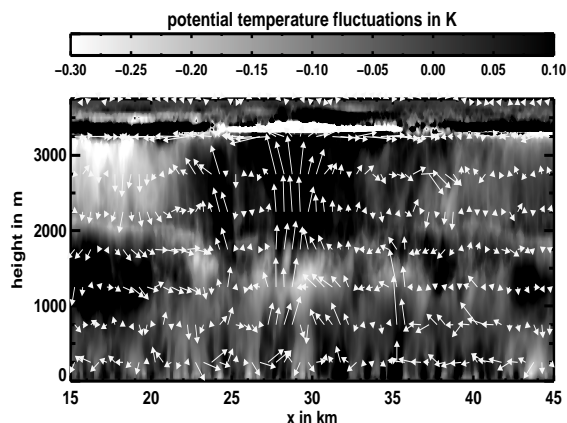


Figure 5: Contour plots of the potential temperature fluctuations and a vector plot of the averaged velocity field for a vertical x - z cross section at $y = 20$ km and $t = 12.5$ h. Temperature fluctuations are obtained by subtracting the corresponding horizontal average.

moved by our high resolution / large domain study. In order to point out the correlation between the dynamics of the flow and its thermodynamics (temperature and liquid water content) Figure 5 presents a cross section in the x - z -plane through a single convective cell. Shown are isopleths of temperature fluctuations for $y = 20$ km (see Fig. 1b). Additionally the flow dynamics are indicated by mean velocity vectors (u, w averaged over five grid points). Due to the latent heat release during the condensation process the temperature increases (dark areas for $2000 \text{ m} < z < 3200 \text{ m}$). Correspondingly in areas with descending air, temperature decreases due to evaporation ($x \approx 15$ - 20 km). Together these areas of ascending and descending air form the circulation of the mesoscale convective cells. This large scale homogeneous distribution of temperature fluctuations in the sub-cloud layer is in accordance with the results of Jonker et al. (1999b).

4 MECHANISMS OF CELL BROADENING

Although the conditions necessary for cell broadening now seem to be definitely clarified, a satisfactory proved explanation for the physical mechanism which leads from the release of latent heat and radiative cooling to final cell broadening is still missing. Müller and Chlond (1996) state that the additional cooling of downdrafts by radiation processes increases the aspect ratio because it increases the horizontal distance which has to be passed by the horizontally outflowing downdraft air before the air becomes positively buoyant. We

believe that this argument is not convincing because an increased temperature difference between the sea and the overlying air increases the surface heat flux so that cooler air receives more energy than comparably warmer air reducing its time to become positively buoyant. Additionally, our simulation results show that intensive small-scale updrafts are randomly distributed throughout the whole near-surface layer (see temperature fluctuations in Figure 5).

Dörnbrack (1997) hypothesizes that the additional cooling at the cloud top leads to an increase of the effective horizontal diffusion, which eventually leads to the cell broadening. We actually try to derive horizontal transfer coefficients from our simulation data in order to show that latent heat release in the cloud layer as well as cloud-top radiative cooling are causing a stronger horizontal mixing.

ACKNOWLEDGEMENTS

This project was supported by the Deutsche Forschungsgemeinschaft under contract number RA 617/3-3. All runs were performed on the Cray-T3E LC 384 of the Konrad-Zuse-Zentrum für Informationstechnik in Berlin (ZIB).

REFERENCES

- Atkinson, B. W., J. W. Zhang, 1996: Mesoscale shallow convection in the atmosphere. – *Rev. Geophys.* **34**, 403–431.
- Dörnbrack, A., 1997: Broadening of convective cells. – *Quart. J. R. Meteorol. Soc.* **123**, 829–847.
- Jonker, H. J. J., P. G. Duynkerke, J. W. M. Cuipers, 1999a: Mesoscale fluctuations in scalars generated by boundary layer convection. – *J. Atmos. Sci.* **56**, 801–808.
- Jonker, H. J. J., P. G. Duynkerke, A. P. Siebesma, 1999b: Development of mesoscale fluctuations in cloud topped boundary layers. – In: 13th Symposium on Boundary Layers and Turbulence, pp. 197–200.
- Müller, G., A. Chlond, 1996: Three-dimensional numerical study of cell broadening during cold-air outbreaks. – *Boundary-Layer Meteorol.* **81**, 289–323.
- Raasch, S., M. Schröter, 2001: **PALM** - A large-eddy simulation model performing on massively parallel computers. – *Meteorol. Z.* **10**, 363–372.